Title : will be set by the publisher
Editors : will be set by the publisher
EAS Publications Series, Vol. ?, 2013

FORMATION AND EVOLUTION OF DWARF GALAXIES IN THE CDM UNIVERSE

Lucio Mayer[1]

Abstract. We first review the results of the tidal stirring model for the transformation of gas-rich dwarf irregulars into dwarf spheroidals, which turns rotationally supported stellar systems into pressure supported ones. We emphasize the importance of the combined effect of ram pressure stripping and heating from the cosmic ultraviolet background in removing the gas and converting the object into a gas poor system as dSphs. We discuss how the timing of infall of dwarfs into the primary halo determines the final mass-to-light ratio and star formation history. Secondly we review the results of recent cosmological simulations of the formation of gas-rich dwarfs. These simulations are finally capable to produce a realistic object with no bulge, an exponential profile and a slowly rising rotation curve. The result owes to the inclusion of an inhomogeneous ISM and a star formation scheme based on regions having the typical density of molecular cloud complexes. Supernovae-driven winds become more effective in such mode, driving low angular momentum baryons outside the virial radius at high redshift and turning the dark matter cusp into a core. Finally we show the first tidal stirring experiments adopting dwarfs formed in cosmological simulations as initial conditions. The latter are gas dominated and have have turbulent thick gaseous and stellar disks disks that cannot develop strong bars, yet they are efficiently heated into spheroids by tidal shocks.

1 Introduction

Dwarf galaxies are key to understand galaxy formation as well as the nature of dark matter. Gas-rich dwarfs have slowly rising rotation curves that are reproduced better with dark matter halos having a central core rather than the cuspy profiles predicted by CDM (see the review by de Blok 2010 and Oh et al. 2008 for the recent results of the THINGS survey). These galaxies also have nearly exponential profiles and no central stellar bulges. Cosmological simulations of galaxy

[1] Institute fir Theoretical Physics, University of Zürich, 8057, Winterthurestrasse 190, Zürich

DOI: (will be inserted later)

formation, instead, always produce galaxies with prominent bulges and steep rotation curves, irrespective of the mass scale (Mayer et al. 2008). Dwarf spheroidals (dSphs) in the Local Group are the faintest galaxies known. Including the ultra-faint dwarf spheroidals discovered in the last few years, they span luminosities in the range $-3 < M_B < -14$. At variance with gas-rich dwarfs, they are gas poor and have pressure supported stellar components (Mateo 1998). Among them some stopped forming stars about 10 Gyr ago and other have extended star formation histories (Hernandez et al. 2000; Coleman & de Jong 2008; Orban et al. 2008). They are typically clustered around the largest galaxy in a group, although a few of them are found also at significantly larger distances from the primary galaxy (Mateo 1998). These properties of dSphs, while best studied and known in the Local Group due to its proximity, are also typical of this class of galaxies in nearby groups and clusters. Chiboucas, Karachentsev & Tully (2009) have recently uncovered a population of dSphs in the M81 group having a range of luminosities comparable to the LG dwarfs and which share with the latter the same scaling relations between fundamental structural properties, such as the relation between luminosity and effective radius. Recent studies of early-type dwarfs in clusters (Misgeld, Hilker & Mieske 2009) show that there is overlap in the structural properties between the faint spheroidals in clusters and the classic dSphs in the LG, as shown by the size-luminosity and the surface brightness-luminosity relations. Strong similarities between dSphs in the LG and in clusters are also found by Penny et al. (2009) in their study of the Perseus cluster. Hence, LG dSphs can be considered as a representative laboratory for the study of dSphs in the Universe. In this paper we review the substantial progress made over the last years in two areas. First, we summarize results of a scenario in which tidal stirring and ram pressure stripping with the halos of primary galaxies drive the transformation from gas-rich dwarfs to dwarf spheroidals over a few orbits of the dwarf satellites (5-10 Gyr). The we discuss the results of the first high resolution cosmological simulations of dwarf galaxy formation capable of obtaining realistic rotation curves and suppress bulge formation. Finally we conclude with outlining work in progress that aims at combining both scenarios.

2 Tidal stirring, ram pressure stripping and the timing of infall into the primary: the transformation of dIrrs into dSphs

Mayer et al. (2001a,b), Klimentowski et al. (2007;2009a) and Lokas et al. (2010) have shown that low surface brightess disky dwarfs are turned into pressure supported spheroidal systems as a result of repeated tidal shocks at pericenter passages as they orbit within the primary halo. The timescale of the transformation is a few orbital times (several Gyr). The mechanism behind the transformation is tidally induced non-axisymmetric instabilities of stellar disks combined with impulsive tidal heating of the stellar distribution. The typical orbits considered are consistent with those of satellites in cosmological simulations, having an apocenter to pericenter rauo of 5-6.

We recall that the time-dependent tidal field varies on a timescale proportional

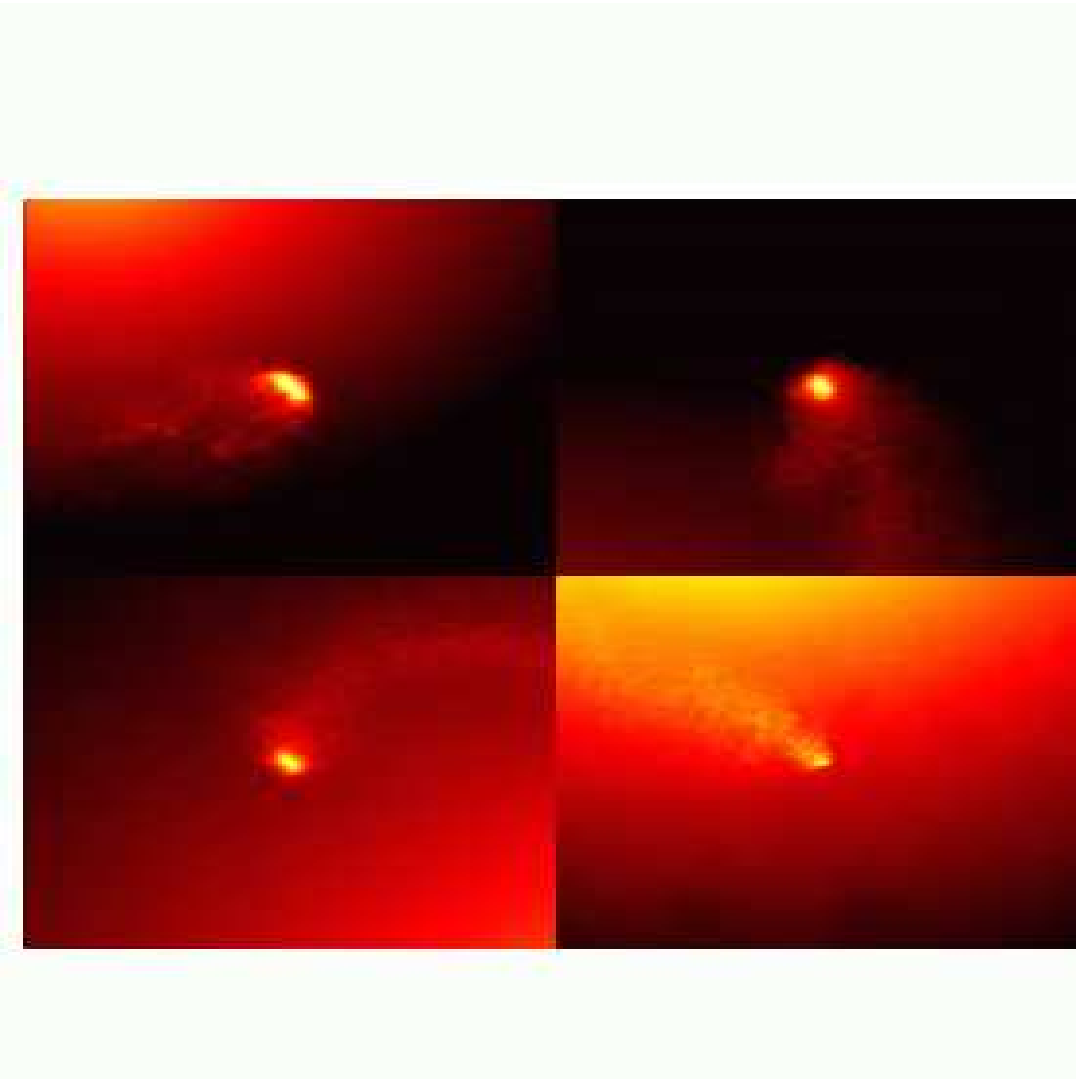

Fig. 1. Evolution of the gas-dominated disky dwarf model studied in Mayer et al. (2007), which produces a dark matter dominated dwarf resembling Draco after 10 Gyr of evolution. This N-Body + SPH simulation employed millions of dark matter, gas and star particles. It included tidal mass loss due to a live Milky Way halo, ram pressure stripping in a tenuous gaseous halo, radiative cooling and a time-varying cosmic ionizing UV background consistent with the Haardt & Madau (2000) model. The snapshots show the color coded logarithmic density maps (the brighter the color the higher the density, with densities in the range $10^{-32} - 10^{-23}$ g cm-3) for the first 2.5 Gyr of evolution. Boxes are 30 kpc on a side. The dwarf begins falling into the Milky Way halo on a typical eccentric cosmological orbit (apo/per= 5 at the beginning of the simulation, which corresponds to $z = 2$). At the first pericenter passage ($R_{peri} = 30$ kpc) a prominent ram pressure tail is evident (top left), and once the dwarf comes to first apocenter (top right) it has lost already more than half of its gas. As it begins the second orbit ram pressure stripping continues to remove gas (bottom left), until all gas is stripped at second pericenter (bottom right).

to the orbital timescale of the galaxy. In simulations of disky dwarfs on eccentric orbits interacting with a Milky Way-sized halo the following sequence of events is typically observed. First, tidal shocks induce strong bar instabilities in otherwise stable, light disks resembling those of present-day dIrrs. Second, the bar buckles due to the amplification of vertical bending modes and turns into a spheroidal component in disks with relatively high stellar surface density (Mayer et al. (2001a,b), or else subsequent shocks destroy the centrophilic orbits supporting the bar which then loses its elongation and heats up into a more isotropic diffuse spheroid (Mayer et al. 2007; Klimentowski et al. 2009a). The second channel for the transformation is favoured in systems with lower mass, lower surface density disks; for these tidal heating is particularly efficient because the dynamical response of the stellar system is impulsive rather than adiabatic. Kazantzidis et al. (2011) have shown, by exploring a wide parameter space, that both the pericenter distance and the orbital time are the key parameters that set the efficiency of the transformation (see the paper for a detailed discussion). The stars lose angular momentum as the bar instability arises, transferring it to the outer regions, that are mostly tidally stripped. The result is thus a system with a low v/σ, below 0.5, consistent with dSphs. Mayer et al. (2006) studied the combined effect of ram pressure and tidal stripping, showing how only when both are considered simultaneously is the original gas content of the dwarf irregular progenitor removed in a few Gyr (a couple of orbits). This result was obtained assuming that a primary galaxy such as the Milky Way has hot gaseous halo with density a few times 10^-5 atoms/cm^3 at 50 kpc, with a power-law profile, consistent with various observational constraints.

In Mayer et al. 2007 we built on the results of Mayer et al. (2001a,b) and Mayer et al. (2006) and proposed a coherent scenario that explains at the same time the origin of the common properties of dSphs (low gas content, exponential profiles, low luminosity and surface brightness, low angular momentum content) and their differences (different star formation histories and mass-to-light ratios). In this model the key parameter is the epoch of accretion onto the Milky Way and a key assumption is that the progenitors of present-day classic dSphs were not simply gas-rich but extremely gas dominated, consistent with what is found in most present-day dIrrs in the Local Group and elsewhere in the nearby Universe (Geha et al. 2006). The large gas fractions found in field dwarfs can be understood in terms of a decreasing star formation efficiency towards decreasing galaxy mass. Recently, the THINGS survey (Leroy et al. 2008) has confirmed that disky dwarfs have a star formation efficiency, defined as the fraction of gas (atomic+molecular) that is converted into stars, well below that of normal spirals. The low gas surface densities typically found in dwarfs likely imply a low conversion efficiency between atomic hydrogen and the star forming molecular hydrogen phase (Schaye 2004), probably explaining the low star formation efficiency. Such conversion can be even less efficient in presence of the ionizing ultraviolet flux arising during reionization, which can dissociate molecular hydrogen (Schaye 2004). Therefore for field dwarfs that were accreted by the Milky Way or M31 at $z > 1$ the assumption of mostly gaseous baryonic disk is even more well grounded.

The initial conditions, including the orbits of the satellites, were chosen based

on a hydrodynamical cosmological simulation of the formation of a Milky Way-type galaxy (Governato et al. 2007). We found that satellites that were accreted when the cosmic ionizing background was still high, roughly before $z = 1$, were completely ram pressure stripped of their gas in one to two pericenter passsages (Figure 1). As a result their star formation was truncated. The effect of the ionizing radiation is to heat and ionize the gas, making it more diffuse because of the increased pressure support, and to suppress star formation. This, in turn, makes it easier to strip even from the central regions of the dwarf, essentially having the same effect of a reduced binding energy. Hence gas-rich dwarfs accreted when the UV radiation background was at its peak lost most of their baryonic content because this was initially in gaseous form, thus naturally ending up with a very low luminosity. While their baryonic content dropped orders of magnitude below the cosmic mean as a result of gas stripping, their original central dark matter mass in the central region around the surviving baryonic core was largely preserved because dark matter is affected only by tides, not by ram pressure. This automatically produced very high mass-to-light ratios, of order 100 (see Figure 2 in Mayer et al. 2007). We showed that all the final properties of such systems after 10 billion years of evolution, including the stellar velocity dispersion profiles, resemble those of the classic strongly dark matter dominated dwarfs such as Draco, Ursa Minor or And IX. Even the brightest among the ultra-faint dwarfs, that have velocity dispersions > 5 km/s (e.g. Ursa Major) may be explained by this model. However, the very low characteristic mass scale of most ultra-faint dwarfs suggests that other formation paths might indeed be more likely.

Dwarfs that fell into halos of bright galaxies below $z = 1$, when the cosmic UV radiation dropped by more than an order of magnitude, retained some gas because tides and ram pressure could not strip it completely, and underwent subsequent episodes of star formation at pericenter passages due to bar-driven inflows and tidal compression (Mayer et al. 2001a,b). These ended up in dSphs that are brighter for a given halo mass (or given central stellar velocity dispersion) compared to the ones that were accreted earlier. This is should be case with e.g. Fornax, Carina or Leo I. The two regimes of infall epochs explain why Fornax and Draco have roughly the same halo peak circular velocities (and thus mass) despite having a luminosity and mass-to-light ratio that differs by about an order of magnitude. Likewise, Carina and Leo I, these being prototypical cases of dSphs with an extended (episodic) star formation history, have a luminosity comparable to Draco but a mass-to-light ratio 5-10 times lower than that of Draco (Mateo 1998).

As a final remark, we note that Madau et al. (2008) argue that a very low efficiency of star formation, corresponding to less than 0.1% of their total mass being converted into stars, would offer a solution to the excess in number counts of subhalos with $V_c > 20$ km/s in dark matter-only simulations (see also Koposov et al. 2009 for a similar interpretation). Our model for the origin of Local Group dwarf spheroidals provides a clue to why dSphs were so inefficient at producing a stellar component, thus pointing to a solution of the substructure problem at the bright end of the mass function of dwarf satellites of the Milky Way, which essentially contains all the classic dSphs. Instead of relating the low efficiency

of star formation to photoevaporation and/or suppression of gas accretion by the cosmic ultraviolet background, we argue that it arose naturally from intrinsic low star formation efficiency in the progenitor gas-rich dwarfs (well below 1% - see also Robertson & Kravtsov 2008) combined with copious gas stripping after they were accreted in the potential of the primary galaxy. Our mechanism is absolutely general in hierarchical structure formation and should thus apply to dwarf galaxy satellites of any galaxy group. The combination of an intrinsic low star formation efficiency prior to infall with ram pressure and tidal stripping can be thought of as an effective feedback mechanism alternative to reionization and supernovae feedback.

3 The formation of a realistic dwarf galaxy; inhomogeneous ISM and supernova-driven outflows

Here we focus on one important aspect of the recent paper Governato et al. (2010), in which we showed for the first time the formation of a realistic dwarf galaxy in a cosmological simulation of the concordance (WMAP5) cosmology. We refer to the paper for the technical details of the simulations. Several analytical and numerical papers have highlighted the necessity of resolving a clumpy multi-phase ISM to achieve a realistic modeling of energy deposition in the central regions of galaxies. While using a variety of arguments, these works suggest that only in a clumpy ISM is it possible to a) transfer orbital energy from gas to the DM as dense clumps sink through dynamical friction or resonant coupling (Mashchenko et al. 2006,2008;Binney et al.2001;Mo & Mao 2004, El-Zant et al. 2004) and have b) efficient gas outflows (Maller & Dekel 2002,. In turn, these outflows 1) suppress the formation of stellar bulges by removing negative or low angular momentum gas (Van den Bosch et al. 2001; Binney et al. 2001) and 2) make the central DM expand by suddenly reducing the total enclosed mass and reducing the DM binding energy (Navarro, Eke & Frenk 1996; Mo & Mao 2004; Read & Gilmore 2005). However, none of the above works has simultaneously studied the formation of bulgeless galaxies and that of DM cores, even if they both are crucial properties of small galaxies.

In order to achieve a multi phase ISM numerical works agree that a minimal spatial resolution of about 100 pc is required, and that SF has to be associated with dense regions with gas density ($\sim$ 100 amu/cm^3) (Robertson & Kravtsov 2008; Saitoh et al. 2008). Our simulations satisfy both conditions and unify the many proposed models that focused on different aspects of the problem to robustly demonstrate that energy transfer and subsequent baryon removal are concurrent and effective to create bulgeless galaxies with a shallow DM profile in a full cosmological setting.

To illustrate the clumpiness of the ISM in our simulations, Figure 2 highlights the differences in the density distribution of the interstellar medium between the simulations DG1MR and DG1LT (see Table 1), by plotting the local gas density vs radius of each gas particle at a representative epoch of z=0.75. These two runs have the same mass and spatial resolution and adopt identical feedback schemes.

They only differ in the way regions where SF happens are selected. In the "high threshold" runs (DG1,DG2 DG1MR and DG1LR) SF happens only in regions above a high gas density threshold (100 amu/cm^3, the horizontal red line in the left panel of Figure 2). The density peaks then correspond to isolated clumps of cold gas with masses and sizes typical of SF regions. The efficiency of SF, ϵSF, for these regions must be increased from 0.05 (LT) to 0.1 (HT) in order to match the observed normalization of SF density in local galaxies. However, due to the increased densities, at any given moment only a few regions are actively forming stars. These star forming regions get disrupted after the first SNe go off and only a small fraction of gas has been turned into stars. Feedback then creates an ISM with cold filaments and shells embedded in a warmer medium. This patchy distribution allows the hot gas to leave the galaxy perpendicular to the disk plane at velocities around 100 km/s. Rather than developing a clumpy ISM as in the "high threshold" case, SF in the "low threshold" scheme is spatially diffuse (Figure 2). This means that SN energy is more evenly deposited onto the gas component, but less overall gas is effected by SN feedback due to the low densities in the SF regions. By monitoring where SN energy is deposited and where gas gets substantially heated at high instantaneous rates, we verified that in the "high threshold" case a larger mass of gas achieves temperatures higher than the virial temperature ($T_{vir} \sim 10^5$ K) per unit mass of stars formed than in the "low threshold" scheme. Since less mass is affected in the "low threshold" scenario, the outflows are weak compared to the "high threshold" case. By z=0 DG1LT has formed ten times more stars, most of them in the central few kpcs, causing strong adiabatic contraction of the DM component. Its light profile is consistent with a B/D ratio of 0.3, typical of much more massive galaxies and more concentrated than in real dwarfs.

We note that in the runs adopting the "high threshold" SF, feedback produces winds that are comparable in strength to those happening in real galaxies of similar mass. However, in our simulations the cold ISM is still only moderately turbulent ($\sim$ 10 km/s at z=0), consistent with observations (Walter et al. 2008), and the galaxies match the observed stellar and baryonic Tully Fisher relation (Blanton et al. 2008), as the SF efficiency is regulated to form an amount of stars similar to that of real dwarf galaxies of similar rotation velocity, as demonstrated by the parallel analysis done by the THINGS team to compare mock observations of DG1 and DG2 with dwarf galaxies in the THINGS survey (Oh et al. 2011).

The different ISM structure and, consequently, the different local strength of supernovae drive outflows, produces dramatic differences in the final mass distribution and rotation curves (Figure 3). Only in the high resolution, high SF density threshold runs the resulting rotation curve is slowly rising, corresponding to the absence of a bulge and a dark matter profile that is cored rather than cuspy as a result of impulsive heating of the dark matter from supernovae ouflows (Read & Gilmore 2005) and transfer of energy and angular momentum of gas clumps to the dark matter background (see the Online Supplementary Information of Governato et al. (2010) and the detailed kinematical analysis performed in Oh et al. 2011 exactly as for the dwarfs in the THINGS survey).

4 Tidal stirring of thick, turbulent disky dwarfs forming in cosmological simulations

In the previous sections we have summarized the tidal stirring scenario for the transformation of dwarf irregulars into dwarf spheroidals and we have discussed the results of the first cosmological simulations describing t he formation of realistic dwarf galaxies. The latter produce galaxies whose mass distribution resembles closely that of dwarf irregulars and late-type dwarfs of the THINGS sample (Oh et al. 2011), with faint low surface brightness disks and slowly rising rotation curves. The shape of the rotation curve, which matches closely observed ones, is the result of three key factors; a realistic baryonic disk with a baryon fraction well below universal and a low central density, the absence of a bulge component and the fact that the dark halo is not cuspy, rather has a shallow inner power law density profile. Of these properties only the first two are satisfied by construction in the ICs normally used in tidal stirring works. At z=0 the galaxy has a peak circular velocity in the range 50-60 km/s, only slightly larger to that used in eg initial conditions of tidally stirred dwarfs that can match the properties of classical dSphs such as Draco and Ursa Minor (Mayer et al 2007). The dwarf galaxies produced in cosmological simulations, simlarly to real dIrrs, have thick stellar and gaseous disks (aspect ratio close to 3:1), a consequence of the turbulent motions triggered by supernovae winds and outflows in the gas and then inherited by the newly born stars. This is inevitable in scenario in which supernovae outflows are so strong to eject more than half of the baryons and alter the slope of the dark matter distribution Sanchez-Janssen et al. (2010) show that dIrrs have normally thick disks. Low mass galaxies with circular velocities lower than 50 km/s are expected to be thick as a natural result of the balance between thermal energy, gravitational binding energy and rotational energy for standard halo spin parameters (Kaufmann et al. 2007). Conversely, model galaxies for tidal stirring, employ a thin disk for both the stellar and gaseous component , with aspect ratio 10:1 (Mayer et al. 2001). Gaseous disks can become much thicker as a result of the heating by the cosmic UV background (Mayer et al. 2006), with aspect ratios even as low as 3:1 , but the inital stellar disk can only be thickened by tides, hence only after the interaction with the main galaxy has begun.

At comparable mass of the disk and halo, which determine the depth of the potential well and hence the strength of the gravitational restoring force, a thicker disk will have a higher vertical stellar velocity dispersion. As a result, it will have a lower self-gravity. Perturbations of the stellar surface density field such as the bar-like modes, should grow less efficiently. For isolated systems and weak perturbations modifications of the standard Toomre analysis show that the critical Toomre Q parameter for axisymmetric modes is lower than unity (close to 0.67, see eg Nelson et al. 1998). Here we show preliminary results of new tidal stirring simulations that employ directly the cosmological dwarfs in the Governato et al. (2010) paper. These are the first hydrodynamical simulations that explore tidal interactions using an hybrid approach, namely combining the very high resolution proper of idealized binary interaction experiments with cosmological initial condi-

tions for one of the two galaxies (the dwarf satellite in this case). The DG2 dwarf is extracted at two different cosmic epochs during the simulations (z=2 and z=1) and implanted in the same multi-component model of the Milky Way used in the experiments of Mayer et al. (2006, 2007) and reviewed in section 2, which includes a hot gaseous corona, and therefore allows to model the effect of ram pressure. The adopted eccentric orbit is similar to that chosen by Mayer et al. (2007).

The two different extraction epochs correspond effectively to two different dwarf models; not only the dwarf grows in mass from z=2 to z=1, but also changes in structure, becoming more rotationally supported owing to accretion of higher angular momentum material, acquiring a shallower halo density profile, yet maintaining a fairly high thickness. Figure 5 shows the first results of the simulation adopting DG2 extracted at z=1, with the dwarf caught soon after the first pericenter passage. At this time the dwarf has a peak circular velocity of about 45 km/s, similar to that of the Mayer et al. (2007) ICs, it is gas-dominated and has already a slope shallower than NFW. Ram pressure stripping has already removed the outer gas disk. As shown in the Figure the disk is tidally distorted but there is no sign of the strong bar-like mode ubiquitous in previous tidal stirring runs at the same stage. Yet the disk has been heated into a spheroid and v/σ is lower than 0.5 near the end of the second orbit, which is how far the run has progressed so far, having decreased by almost a factor of 4 relative to the initial state. It appears that direct tidal heating is the culprit behind the transformation rather than tidally induced non-axisymmetric instabilities. Kazantzidis et al. (2011), that have completed the largest parameter survey for tidally stirred dwarfs starting with equilibrium models, find that disk thickness had little effect on the transformation. In the latter work the amplitude of the bar mode decreases faster after the first orbit in the thicker disk case, but the bar is forming nevertheless, and the final state was extremely close to that of models with disks even three times thinner. The thick disk case had a disk scale height about a third of the scale length, not far from the cosmological dwarf. Therefore the reason why the bar does not form in the cosmological dwarf cannot be simply traced to the thicker disk, rather other structural properties might play a role in combination to it. One important difference is that the cosmological dwarf has a disk which is gas dominated rather than purely stellar as in Kazantzidis et al. (2011), which further decreases the stellar disk surface density and its response to the tidal perturbation. Mayer et al. (2007) considered gas dominated dwarfs but with initially thin stellar disks (aspect ratio ~ 0.1); the bar was forming at first pericenter but was dissolving soon afterwards, and direct tidal heating was then taking over. It is thus possible that a disk that is both gas dominated and thick the response is so weak that the bar does not arise at all. A detailed analysis of the evolution of the Toomre and swing amplification parameters will shed light on this. It will be performed in a a forthcoming paper. Therefore, we expect this new work will confirm the tidal sirring scenario for dwarfs forming in a cosmological context, but will also show that non-axisymmetric instabilities are not as crucial as previously found in driving the transformation.

Run	M_i	$g-r$	SFR $M_\odot$/yr	R_s i kpc	V_{rot} km/s	M_{HI}/L_B
DG1	-16.8	0.52	0.01	0.9	56	1.2
DG1MR	-16.9	0.54	0.02	0.9	55	1.0
DG1LR	-18.7	0.33	0.22	0.9	62	0.64
DG1LT	-19.4	0.40	0.38	1.3	78	0.11
DG2	-15.9	0.46	0.02	0.5	54	2.8

Summary of the observable properties of the different dwarf runs. the SFR is in M$\odot$/yr, R_s is the disc scale length, V_{rot} is measured using t

References

Binney, J., Gerhard, O., & Silk, J., 2001, MNRAS, 321, 471

Blanton, M.R., Geha, M., & West, A.A., 2008, ApJ, 682, 861

Chiboucas, K., Karachentsev, D., & Tully, R.B, 2009, ApJ, 137, 3009

Coleman, M. & de Jong, J.T., 2008, ApJ, 685, 946

de Blok, W.J.G., 2010, Advances in Astronomy, 789293

El-Zant, A. et al,, 2004, ApJL, 607, L75

Geha, Blanton, M. R., Masjedi, M., West, A. A., 2006, ApJ, 653, 240

Governato, F., Willman, B., Mayer, L., Brooks, A., Stinson, G., Valenzuela, O., Wadsley, J., Quinn, T., 2007, MNRAS, 374, 1479

Governato,F., Brook, C., Mayer, L., et al., 2010, Nature, 463, 203

Haardt, F., & Madau, P., 1996, ApJ, 461, 20

Hernandez, X., Gilmore, G., & Valls-Gabaud, D. 2000, MNRAS, 317, 831

Kazantzidis, S., et al., 2011, ApJ, 726, 98

Kaufmann, T., Wheeler, C., & Bullock, J., 2007, MNRAS, 375, 53

Klimentowski, J., Lokas, E.L., Kazantzidis, S., Prada, F., Mayer, L., & Mamon, G., 2007, MNRAS, 378, 353

Klimentowski, J., Lokas, E.L., Kazantzidis, S., Mayer, L., & Mamon, G., 2009a, MNRAS, 397, 2015

Klimentowski, J., Lokas, E.L., Kazantzidis, S., Mayer, L., Mamon, G., & Prada, F., 2009b, MNRAS, in pres

Leroy, A., Walter, F., Brinks, E. Bigiel, F., de Blok, W. J. G., Madore, B., Thornley, M. D., 2008, AJ, 136, 378

Lokas, E., Kazantzidis, S.,Klimentowski, J., & Mayer, L., & Callegari, S., 2010, ApJ, 708, 1032

Madau, P., Kuhlen, M., Diemand, J., Moore, B., Zemp, M., Potter, D., Stadel, J., 2008b, ApJ, 689, L41

Maller, A., & Dekel, A., MNRAS, 2002, 335, 487

Mashchenko, S., Wadsley, J., & Couchman, H., 2008, Science, 319, 974

Mateo, M., 1998, ARA&A, 36, 435

Mayer, L., Governato, F., Colpi, M., Moore, B., Quinn, T., Wadsley, J., Stadel, J., Lake G. 2001a, ApJ, 547, L123

Mayer, L., Governato, F., Colpi, M., Moore, B., Quinn, T., Wadsley, J., Stadel, J., Lake G. 2001b, 559, 754

Mayer, L., Moore, B., Quinn, T., Governato, F., & Stadel, J. 2002, MNRAS, 336, 119

Mayer, L., Mastropietro, C., Wadsley, J., Stadel, J., & Moore, B., 2006, MNRAS,369, 1021

Mayer, L., Kazantzidis, S.; Mastropietro, C.; Wadsley, J., 2007, Nature, 445, 738

Mayer, L., Governato, F., Kaufmann, T., 2008, ASL, 1, 7

Misgeld, I., Hilker, M., & Mieske, S., 2009, A&A, 496, 683

Mo, H. & Mao, S. 2004, MNRAS, 353, 829

Oh, S.H., et al. 2008, MNRAS, 136, 276

Navarro, J. F., Eke, V. R., & Frenk, C.S., 1996, MNRAS, 238, L72

Oh, S.H., et al., 2011, AJ, in press, 2010arXiv1011.2777O

Orban, C., *et al.*, 2008, ApJ, 686, 1030

Penny, S.J., et al., 2009, MNRAS, 393, 1054

Read, J.I., & Gilmore, G., 2005, MNRAS, 356, 107

Robertson, B., & Kravtsov, A., 2008, ApJ, 680, 1083

Saitoh, T.R., et al., 2010, PASJ, 60, 667

Sanchez-Janssen, R., Mendez-Abreu, J,. & Aguerri, J.A.L., 2010, MNRAS, 406, L65

Schaye, J., 2004, ApJ, 609, 667

Tasker, E., J., & Bryan, G.L., 2008, ApJ, 673, 810

Van den Bosch, F.C., Burkert, A. & Swaters, R.A, 2001, MNRAS, 326, 1205

Walter, F., et al., 2008, ApJ, 136, 810

Zavala, J., Okamoto, T., & Frenk, C.S, 2008, ApJ, 387, 364

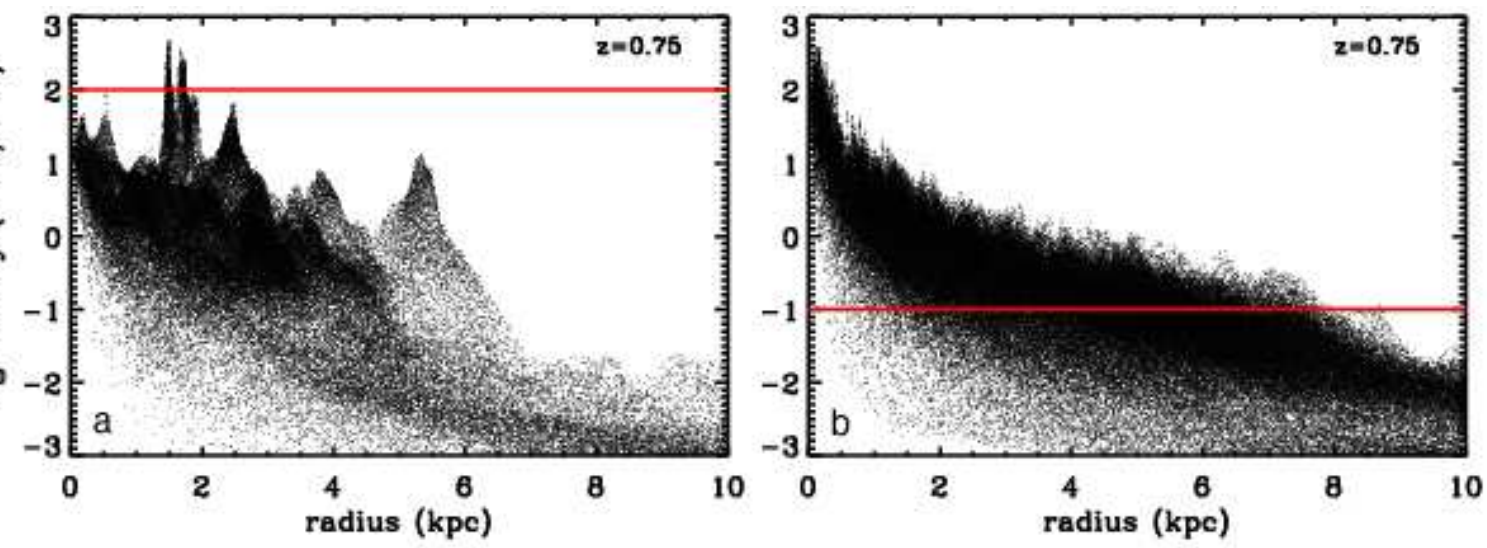

Fig. 2. Properties of the gas distribution for different SF implementations. The local gas density measured around each SPH particle is plotted as a function of its radial distance from the galaxy center for runs DG1MR and DG1LT, which have identical force and mass resolution, but differ in the star formation density threshold. Horizontal red lines mark the minimum gas density for SF in each run. In both runs the SFR is $\propto {\rho_{gas}}^{1.5}$. In the low threshold simulation, diffuse star formation in the inner regions continues unabated by feedback, as SN energy is more evenly distributed and is unable to originate major outflows. Allowing star formation only in high density regions results in a complex, inhomogeneous ISM, even in the central regions and fast outflows that remove gas preferentially from the galaxy center.

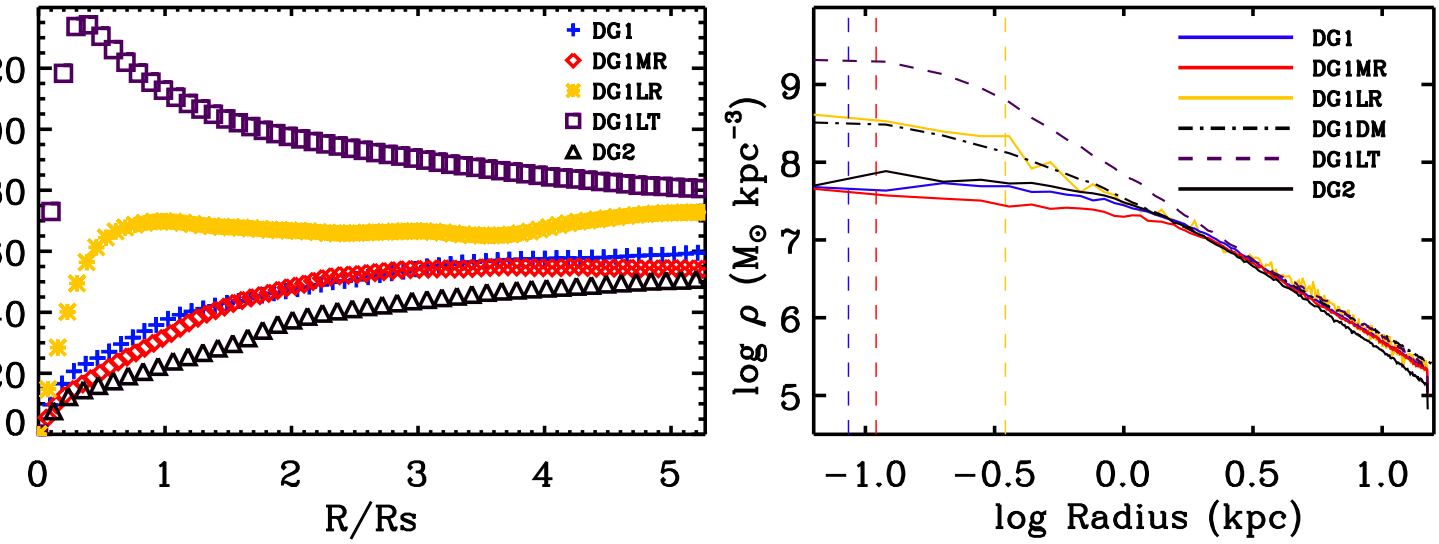

Fig. 3. The rotation curve and DM radial distribution of the models described in §3 and §5, to show the effects of resolution and different SF recipes on the central mass distribution of simulated dwarf galaxies. The left panel shows the rotation curve, derived using the 3D potential of each galaxy and measured at z=0, for DG1 (blue crosses), DG1MR (red diamonds) and DG1LR, (yellow stars), plotted versus the disc scale length (1kpc for DG1, 0.5kpc for DG2). The three runs use the same gas density threshold for SF (100 atoms/cm^3), but MR and LR runs use only 40% and 12.5% of the particles of the reference run (with particle masses rescaled to the same total mass), and a softening respectively 1.33 and 4 times larger. Results have converged at the DG1MR resolution, while the LR run shows an excess of central material that is due to poor resolution causing artificial angular momentum loss (Mayer et al. 2008). The squares show DG1LT, where star formation is allowed in regions with a much lower local density (0.1 atoms/cm^3), again resulting in a much higher central mass density, due to the lack of outflows. This result demonstrates that the correct modeling of where SF is allowed to happen (namely only in gas with density comparable to that of real star forming regions) is crucial to obtain the results described in Governato et al. 2010 and summarized here. The rotation curve of galaxy DG2 (black triangles) shows the same shape as that of the DG1 run. Panel B uses a similar colour scheme and plots the DM density profile for the same runs. DG1 (blue solid), DG1MR (red dashed) show similar profiles, with a DM core of about 1kpc. Color coded vertical lines mark the force resolution for each run. The DM only run DG1DM (dot dashed), shows instead a cuspy profile down to the force resolution (red dashed vertical line as for DG1MR). The central density is about 10 times higher than in the runs with strong outflows. DG2 has a similar profile to DG1, while the lower resolution run or the run with diffuse SF have dense and cuspy DM profiles down to the force softening length.

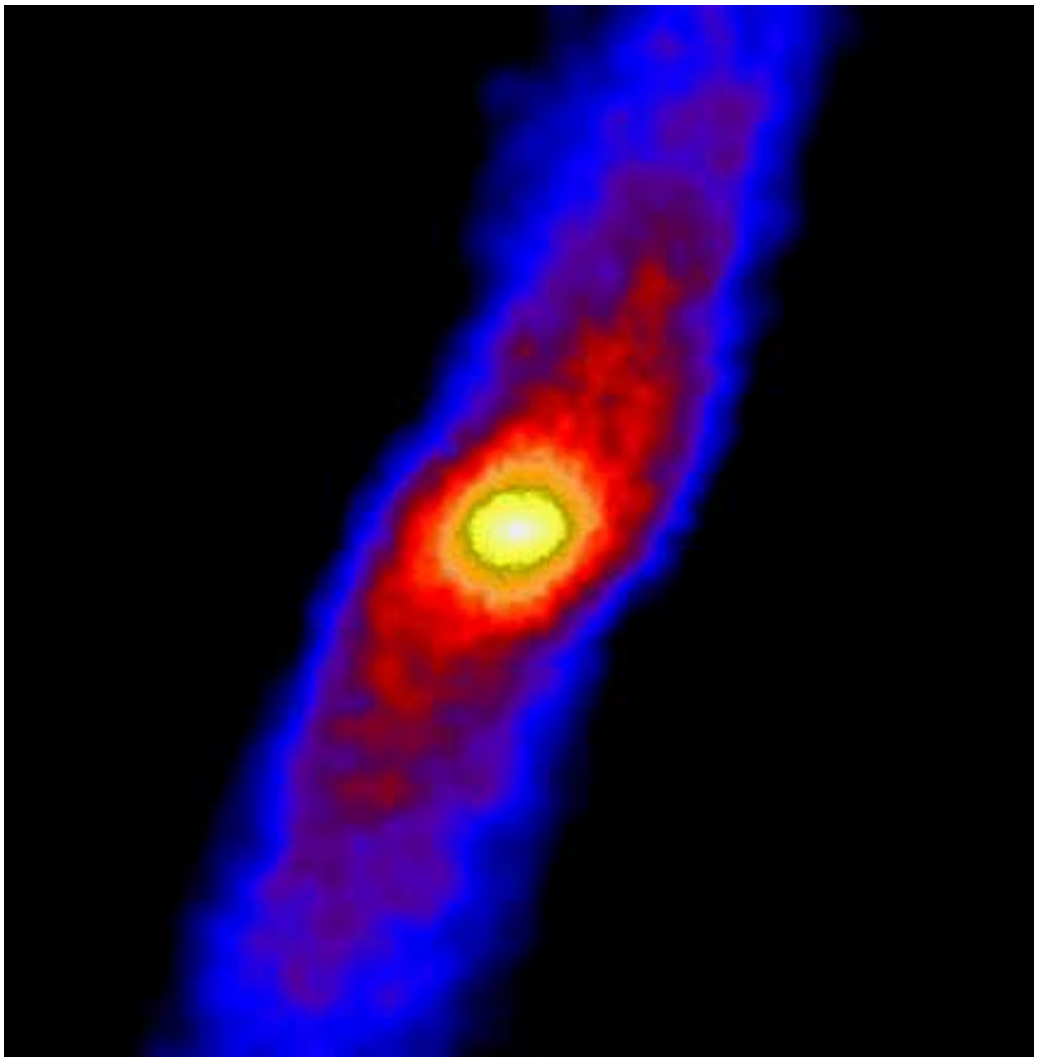

Fig. 4. Evolved state of the cosmological dwarf DG1 extracted at z=1 and placed on orbit inside a live Milky Way model. The color-coded density map of the stars seen face-on (perpendicular to the angular momentum vector) is shown. The dwarf is displayed after first pericenter passage. The tidal distorion is evident but there is no sign of a strong bar